Acta Crystallographica Section D
Biological Crystallography
ISSN 0907-4449

Flexibility of the flap in the active site of BACE1 as revealed by crystal structures and molecular dynamics simulations

Yechun Xu,[a,b,c]*‡ Min-jun Li,[b]‡ Harry Greenblatt,[b] Wuyan Chen,[a] Aviv Paz,[b,c] Orly Dym,[b,d] Yoav Peleg,[b,d] Tiantian Chen,[a] Xu Shen,[a] Jianhua He,[e] Hualiang Jiang,[a,f] Israel Silman[c,d] and Joel L. Sussman[b,d]*

[a]Drug Discovery and Design Center, Shanghai Institute of Materia Medica, Chinese Academy of Sciences, 555 Zuchongzhi Road, Shanghai 201203, People's Republic of China, [b]Department of Structural Biology, Weizmann Institute of Science, Rehovot 76100, Israel, [c]Department of Neurobiology, Weizmann Institute of Science, Rehovot 76100, Israel, [d]Israel Structural Proteomics Center, Weizmann Institute of Science, Rehovot 76100, Israel, [e]Shanghai Institute of Applied Physics, Chinese Academy of Sciences, Shanghai 201800, People's Republic of China, and [f]School of Pharmacy, East China University of Science and Technology, Shanghai 200237, People's Republic of China

‡ These authors contributed equally to this work.

Correspondence e-mail: ycxu@mail.shcnc.ac.cn, joel.sussman@weizmann.ac.il

Received 10 September 2011
Accepted 8 November 2011

PDB References: BACE1, apo, 3tpj; 3tpl; BSIIV complex, 3tpp; 3tpr.

β-Secretase (β-site amyloid precursor protein-cleaving enzyme 1; BACE1) is a transmembrane aspartic protease that cleaves the β-amyloid precursor protein *en route* to generation of the amyloid β-peptide (Aβ) that is believed to be responsible for the Alzheimer's disease amyloid cascade. It is thus a prime target for the development of inhibitors which may serve as drugs in the treatment and/or prevention of Alzheimer's disease. In the following determination of the crystal structures of both apo and complexed BACE1, structural analysis of all crystal structures of BACE1 deposited in the PDB and molecular dynamics (MD) simulations of monomeric and 'dimeric' BACE1 were used to study conformational changes in the active-site region of the enzyme. It was observed that a flap able to cover the active site is the most flexible region, adopting multiple conformational states in the various crystal structures. Both the presence or absence of an inhibitor within the active site and the crystal packing are shown to influence the flap's conformation. An open conformation of the flap is mostly observed in the apo structures, while direct hydrogen-bonding interaction between main-chain atoms of the flap and the inhibitor is a prerequisite for the flap to adopt a closed conformation in the crystal structures of complexes. Thus, a systematic study of the conformational flexibility of the enzyme may not only contribute to structure-based drug design of BACE1 inhibitors and of other targets with flexible conformations, but may also help to better understand the mechanistic events associated with the binding of substrates and inhibitors to the enzyme.

1. Introduction

Alzheimer's disease (AD), a neurodegenerative disorder, is pathologically characterized by the presence of insoluble amyloid plaques and neurofibrillary tangles in the brain (Selkoe, 1991). The major components of the plaques are amyloid β-peptides (Aβs) consisting of 39–43 residues, which are proteolytically generated from amyloid precursor protein (APP) by consecutive cleavage by β-secretase and γ-secretase or by α-secretase and γ-secretase (Esler & Wolfe, 2001). β-Secretase (β-site amyloid precursor protein-cleaving enzyme 1; BACE1; Vassar, 2004) initiates the cleavage of APP to form a soluble N-terminal ectodomain together with a membrane-bound 99-residue C-terminal fragment (CTF99). The latter is then further processed by γ-secretase to produce Aβ, as well as the APP intracellular domain. BACE1 has been identified as the initial and putatively rate-limiting enzyme in the production of Aβ (Sinha & Lieberburg, 1999). BACE1-knockout mice do not produce β-amyloid and are free of AD-associated pathologies, which include neuronal loss and certain memory

deficits (Cai *et al.*, 2001; Luo *et al.*, 2001; Roberds *et al.*, 2001). BACE1 is therefore a prime target for the development of inhibitors which may serve as drugs for the treatment and/or prevention of AD.

BACE1 [also known as 'Asp 2' (Yan *et al.*, 1999), 'memapsin 2' (Lin *et al.*, 2000) or 'membrane-bound aspartic proteinase' (Sinha *et al.*, 1999)] is a membrane-anchored aspartic protease containing three distinct domains: an N-terminal ectodomain, a single transmembrane domain and a cytosolic C-terminus (Lin *et al.*, 2000). The ectodomain is the protease domain and has the correct topological orientation for cleavage of APP at the sites susceptible to BACE1. The protease domain has a conserved aspartic protease fold, with the substrate-binding cleft located between the N- and C-terminal lobes (Hong *et al.*, 2000; Fig. 1*a*). The conserved catalytic Asp dyad, Asp32 and Asp228 (human numbering), is located at the interface of the two lobes. The hairpin loop in the N-terminal lobe that is known as the 'flap' (residues 67–75) partially covers the cleft and is perpendicular to it, as is generally the case in the aspartic protease family (Hong & Tang, 2004). Conformational changes in the flap are believed to control substrate access to the active site, to position the substrate in the correct geometry for catalysis to occur and possibly to effect removal of the hydrolysis products (Shimizu *et al.*, 2008). A closed conformation in which the flap moves closer to the two-Asp dyad has been observed in the crystal structures of complexes of BACE1 with peptides or with peptide-like inhibitors solved by Tang and coworkers (Hong *et al.*, 2000, 2002; Turner *et al.*, 2005; Ghosh *et al.*, 2005, 2006, 2007, 2008); in apo structures of BACE1 the flap was generally observed to adopt an open conformation as shown in Fig. 1(*a*) (Hong & Tang, 2004; Patel *et al.*, 2004; Shimizu *et al.*, 2008). However, as an increasing number of crystal structures of complexes of BACE1 with nonpeptide inhibitors have been determined in recent years, owing to the strong pharmaceutical interest in development of BACE1 inhibitors, a variety of conformations of the flap have been observed. In addition to these multiple overall orientations of the flap, various side-chain conformations of the conserved flap residue Tyr71, including one that is self-inhibitory, have also been observed in recently solved crystal structures of BACE1 (Gorfe & Caflisch, 2005).

Owing to the significant role of the flap in the function of BACE1 and other aspartic proteases, correlation of its conformational states with enzyme function has been approached in previous structural studies on BACE1 by comparison of the apo crystal structure with those of various complexes (Hong & Tang, 2004; Patel *et al.*, 2004; Shimizu *et al.*, 2008). The conformational flexibility of the flap in both the presence and the absence of inhibitors has also been studied by the use of molecular dynamics (MD) simulations (Gorfe & Caflisch, 2005; Cascella *et al.*, 2005; Xiong *et al.*, 2004). It has been suggested that conformational switching of the flap is highly correlated with binding of inhibitor and that an active conformation of the apo enzyme has a more open structure than an inactive conformation (Shimizu *et al.*, 2008). MD simulations revealed that the flap is very flexible in the absence of the peptidic inhibitor OM99-2 and can switch from an open to a closed conformation or *vice versa* on a 10 ns timescale (Gorfe & Caflisch, 2005).

In the present study, we systematically investigate the flexibility of the flap, making use of several approaches. We compare the different crystal structures obtained by

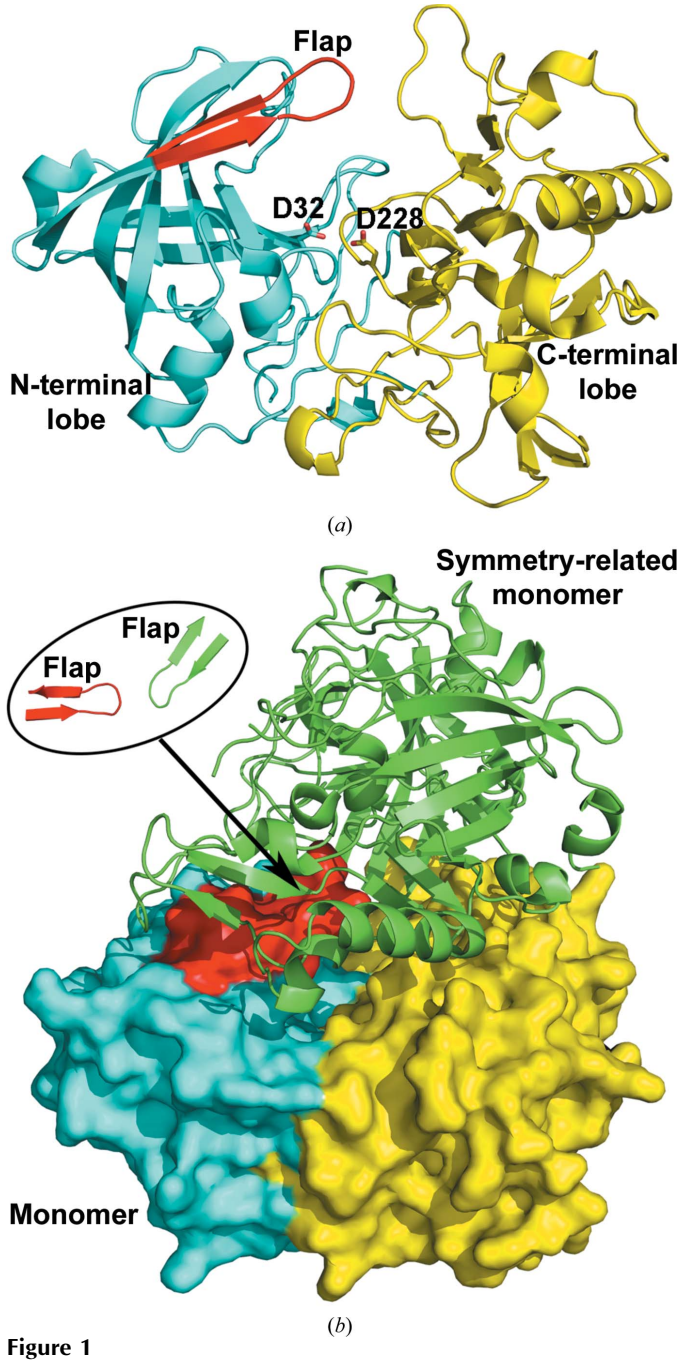

Figure 1
(*a*) Ribbon representation of the three-dimensional structure of apo BACE1. The N- and C-terminal lobes are coloured cyan and yellow, respectively. The Asp-dyad residues, Asp32 and Asp228, are displayed as sticks. Residues 67–78 (including the flap) are coloured red and the flap is shown in its 'open' conformation. (*b*) Ribbon and molecular-surface representations of the three-dimensional structure of the BACE1 'dimer' generated based on PDB entry 1w50. The monomer is displayed in space-filling format. The symmetry-related monomer is displayed in ribbon format. A close-up of two the two flaps in the 'dimer' is displayed in the top left corner.

Table 1
Data-collection and refinement statistics.

Values in parentheses are for the highest resolution shell.

	Soaked crystal	Cocrystallized crystal	Apo1	Apo2
PDB code†	3tpr	3tpp	3tpj	3tpl
Space group	$P6_122$	$C222_1$	$C222_1$	$C2$
Unit-cell parameters				
a (Å)	104.2	104.5	104.4	225.1
b (Å)	104.2	128.2	128.7	105.2
c (Å)	169.6	76.5	76.7	65.1
β (°)				102.05
Wavelength (Å)	0.94	0.87	0.98	0.98
No. of reflections	146152	667868	832307	188470
No. of unique reflections	18273	67247	66612	51694
Resolution range (Å)	50.0–2.55 (2.59–2.55)	50.0–1.60 (1.63–1.60)	50.0–1.61 (1.64–1.61)	46.76–2.50 (2.78–2.50)
Multliplicity	8.0 (8.3)	9.9 (4.4)	12.5 (7.6)	3.6 (3.7)
$\langle I/\sigma(I)\rangle$	31.95 (4.71)	30.13 (2.91)	36.38 (3.69)	6.70 (4.64)
Completeness (%)	98.7 (99.9)	98.8 (87.0)	99.7 (96.2)	96.6 (99.9)
Wilson B (Å^2)	46.51	12.72	15.74	49.36
$R_{\rm merge}$	0.072 (0.490)	0.068 (0.345)	0.086 (0.414)	0.107 (0.277)
Rotation (°)	176	268	360	180
Mosaicity‡ (°)	0.5–0.6	0.3–0.4	0.2–0.4	0.4
$R_{\rm work}/R_{\rm free}$ (%)	22.9/27.3	15.4/18.0	17.7/19.6	21.5/26.4
R.m.s. deviations				
Bond lengths (Å)	0.022	0.028	0.009	0.009
Bond angles (°)	2.023	2.319	1.273	1.174
No. of non-H atoms				
Protein	2796	2993	2945	8503
Inhibitor	41	41	0	0
Water oxygen	85	331	397	98
Others	1 [Cl^-]	62 [2 SO_4^{2-}, 8 Cl^-, 11 urea]	57 [8 SO_4^{2-}, 1 Cl^-, 4 urea]	16 [3 SO_4^{2-}, 1 Cl^-]
Mean temperature factors (Å^2)				
Protein	42.6	14.1	16.7	55.9
Inhibitor	35.2	9.5		
Ramachandran plot, residues in				
Most favoured regions	342 [94.0%]	342 [97.7%]	345 [96.9%]	1040 [94.8%]
Allowed regions	19 [5.2%]	7 [2.0%]	10 [2.8%]	50 [4.6%]
Disallowed regions	3 [0.8%]	1 [0.3%]	1 [0.3%]	7 [0.6%]

† An animated Interactive 3D Complement (I3DC) appears for the four new BACE structures: 3tpr, 3tpp, 3tpj and 3tpl in Proteopedia at http://proteopedia.org/w/Journal:Acta_Cryst_D:1 ‡ The data for Apo2 were processed using *XDS*; the other three data sets were processed using *HKL*-2000.

generating crystals of a complex of BACE1 with the same inhibitor in two different ways and of an apo enzyme with two different crystal-packing patterns, carry out a systematic conformational analysis of all of the currently available crystal structures of BACE1 deposited in the Protein Data Bank (http://www.pdb.org) and perform MD simulations on both the monomer and dimer of BACE1, with crystal packing playing a role in the latter case. We not only study the direct effects of the various inhibitors on the conformation of the flap, but also consider the artifactual restrictions that may arise owing to crystal-packing constraints.

2. Materials and methods

2.1. Protein purification and crystallization

The production of recombinant human BACE1 followed the protocol of Sardana *et al.* (2004) with certain modifications. Briefly, BACE1 was expressed in *Escherichia coli* as inclusion bodies, which were then denatured and refolded into the active monomer. In our case, a cDNA fragment encoding BACE1 residues 43–454 was cloned into pET28a with a TEV protease cleavage site following a six-residue His tag added at the N-terminus. After refolding, nickel beads (Ni Sepharose High Performance, Amersham Biosciences, Uppsala, Sweden) were used to concentrate the protein. The refolding solution was passed through the nickel-bead column (a manually packed column with 10 ml of beads per 3 l of refolding solution) at 2–3 ml min^{-1}. The column was then washed with 20 mM imidazole, 0.5 M urea, 0.5 M NaCl, 20 mM sodium phosphate pH 7.4 (wash buffer) until no further protein could be detected in the eluate using a Bio-Rad protein-assay kit. The refolded BACE1 was then eluted with 300 mM imidazole, 0.5 M urea, 0.5 M NaCl, 20 mM sodium phosphate pH 7.4 (elution buffer). The eluted BACE1 was concentrated using a Vivaspin 20 centrifugal concentrator (Sartorius Stedim Biotech SA, Göttingen, Germany) and injected onto a 124 ml HiLoad Superdex 75 column, from which it was eluted with 1 mM DTT, 0.5 M urea, 150 mM NaCl, 20 mM Tris–HCl pH 7.5, with the monomeric BACE1 eluting at ∼56 ml. In order to obtain crystals with different protein-packing patterns, two mutations, K75A and E77A, were introduced into BACE1 together. Expression and purification of the mutant protein were as for the wild type. BACE1 activity was determined using the BACE1 fluorescence resonance energy-transfer assay kit (Invitrogen, Carlsbad, California, USA). The experimental procedure followed the manufacturer's instructions and the measurements were performed using an Infinite M200 spectrofluorometer (Tecan Group, Männedorf, Switzerland).

The active BACE1 monomer in the elution buffer was concentrated to 8–10 mg ml^{-1} using a Vivaspin 20 centrifugal concentrator. Crystallization of apo BACE1 was performed at room temperature using the hanging-drop vapour-diffusion method by mixing equal volumes of the protein stock solution and precipitant [20–25%(w/v) PEG 5000 monomethyl ether, 200 mM ammonium iodide, 200 mM sodium citrate pH 6.4]. To obtain a crystalline complex with BACE1 inhibitor IV (BSIIV; Merck USA and Canada; catalogue No. 565788), a 5 mM solution of the inhibitor in DMSO was diluted tenfold

to 0.5 m*M* in the precipitant solution to generate a soaking drop. The crystal was transferred into the soaking drop and left for 24 h prior to data collection. Cocrystallization of BSIIV with BACE1 was carried out by mixing a solution of the BACE1–BSIIV complex with an equal volume of precipitant solution (1.5–1.8 *M* Li_2SO_4, 100 m*M* HEPES pH 7.5). The BACE1–BSIIV complex was prepared by adding the inhibitor to the protein solution to a final concentration of 0.5 m*M* BSIIV. Cocrystallization also utilized the vapour-diffusion method in hanging drops. The same cocrystallization protocol was also utilized for another low-affinity inhibitor of BACE1, but resulted in crystals of the apo enzyme. The precipitant solutions used to obtain crystals of apo BACE1 in space groups $C222_1$ (Apo1) and $C2$ (Apo2) were 1.5–1.8 *M* Li_2SO_4, 100 m*M* HEPES pH 7.5 and 16%(*w*/*v*) PEG 8000, 300 m*M* Li_2SO_4, 100 m*M* NaCl, 100 m*M* sodium citrate pH 5.0, respectively. The perfluoropolyether PFO-X175/08 (Hampton Research) was used as a cryoprotectant for all of the crystals.

2.2. Structure determination and refinement

Data were collected at 100 K on beamlines ID14-EH4 (at a wavelength of 0.9395 Å) and ID23-EH2 (at a wavelength of 0.8726 Å) at the ESRF (Grenoble, France) and BL17U (at a wavelength of 0.9793 Å) at Shanghai Synchrotron Radiation Facility (SSRF; Shanghai, People's Republic of China) for the soaked, the cocrystallized and the two apo structures, respectively. The data were processed with the *HKL*-2000 (Otwinowski & Minor, 1997) and *XDS* (Kabsch, 2010) software packages and the structures were solved by molecular replacement using the *CCP*4 program *MOLREP* (Winn *et al.*, 2011). The search model used for the crystals of Apo1 and for the complex obtained by soaking was the apo BACE1 structure (PDB entry 1w50; Patel *et al.*, 2004), while that used for the BSIIV complex and for Apo2 obtained by cocrystallization was the protein monomer from a previously determined crystal structure of the BACE1–BSIIV complex (PDB entry 2b8l; Stachel *et al.*, 2006). The structures were refined using the *CCP*4 program *REFMAC*5 (Winn *et al.*, 2011) combined with the simulated-annealing protocol implemented in the program *PHENIX* (Adams *et al.*, 2002). With the aid of the program *Coot* (Emsley & Cowtan, 2004), BSIIV, water and other molecules were fitted into the initial $F_o - F_c$ maps. The complete statistics, as well as the quality of the solved structures, are shown in Table 1. The four structures have been deposited in the PDB with deposition codes 3tpr, 3tpp, 3tpj and 3tpl (Table 1).

2.3. Analysis of crystal structures

All available structures deposited in the PDB of apo BACE1 and its complexes with inhibitors (145 in total to 10 January 2011) were downloaded and examined (Table S1[1]). The structures belonged to five space groups: $P6_122$, $P12_11$, $P2_12_12_1$, $C222_1$ and $C2$. Six of the data sets, 1sgz (Hong & Tang, 2004), 1w50 (Patel *et al.*, 2004), 2zhs (Shimizu *et al.*, 2008), 2zht (Shimizu *et al.*, 2008), 2zhu (Shimizu *et al.*, 2008) and 2zhv (Shimizu *et al.*, 2008), are those of apo structures, with the rest being those of complexes. Each copy (chain) of BACE1 within the crystallographic asymmetric unit was taken as one conformation for further studies. Data for PDB entries 2q11 (Baxter *et al.*, 2007; chain *C*), 2ze1 (Cole *et al.*, 2008), 3hw1 (Godemann *et al.*, 2009; chain *B*), 3igb (Malamas *et al.*, 2009), 3in4 (Malamas, Barnes, Johnson *et al.*, 2010), 3ine (Malamas, Erdei *et al.*, 2010), 3inf (Malamas, Erdei *et al.*, 2010), 3inh (Malamas, Erdei *et al.*, 2010), 3l38 (Malamas, Barnes, Hui *et al.*, 2010), 3kn0 (Wang *et al.*, 2010; chain *A*), 3l5b (Zhu *et al.*, 2010), 3l5c (Zhu *et al.*, 2010), 3l5d (Zhu *et al.*, 2010; chain *A*), 3l5e (Zhu *et al.*, 2010; chain *B*), 3lnk (Cumming *et al.*, 2010) and 2zjn (Yang *et al.*, 2009) were omitted because some of the residues in the flap or in the 10S loop (near residue Ser10) were observed to be missing. Data for PDB entries 2zjh, 2zji, 2zjj, 2zjk and 2zjl (Yang *et al.*, 2009) were also omitted owing to the fact that key residues either in the flap or at other locations near the active site had been mutated to a cysteine in order to permit the covalent attachment of an inhibitor (Yang *et al.*, 2009). A total of 222 conformations of BACE1 were utilized in the statistical analyses of flap flexibility and of ligand–protein interactions, of which 14 were apo conformations and the remaining 208 were complexes. The 14 apo conformations include not only those in the six apo structures but also those in complexes in which the bound ligand is absent in one of the copies [PDB entries 1xn3 (Turner *et al.*, 2005) chains *A*, *B* and *D*, 3l59 (Zhu *et al.*, 2010) chain *B* and 3hvg (Godemann *et al.*, 2009) chain *C*]. *LIGPLOT* (Wallace *et al.*, 1995) was used to identify and display the hydrogen-bond and hydrophobic interactions between BACE1 and the bound ligand in the 208 complex conformations. The residue numbering adopted for PDB entry 1w50 was used for all other structures.

2.4. MD simulations

The monomer and the 'dimer' that was generated based on the symmetry of crystal packing were both used as starting structures for MD simulations. The single copy of BACE1 in the asymmetric unit of PDB entry 1w50 (space group $P6_122$) was selected as the model for the BACE1 monomer. The model of the BACE1 'dimer' was based on 1w50, which contains only one molecule in the asymmetric unit, using two symmetry-related copies (Fig. 1*b*). The flaps in these two copies are near each other. Within the catalytic dyad, Asp32 is assumed to be protonated and Asp228 to be deprotonated following the published assignments (Park & Lee, 2003; Cascella *et al.*, 2005).

The protocol for building the simulation boxes and the parameter settings for the MD run were the same as in our earlier study (Xu *et al.*, 2008). Briefly, the protein was solvated within a water box and counterions were added to neutralize the whole system. Energy minimizations were carried out before heating the system to 300 K. The AMBER03 force field (Duan *et al.*, 2003) was used for the protein. A 500 ns trajec-

[1] Supplementary material has been deposited in the IUCr electronic archive (Reference: WD5167). Services for accessing this material are described at the back of the journal.

tory was performed for both the monomer and the 'dimer'. The *GROMACS* software package was used for all of the simulations as well as for the trajectory analysis (Berendsen *et al.*, 1995; Lindahl *et al.*, 2001; van der Spoel *et al.*, 2005; Hess *et al.*, 2008).

3. Results

3.1. Crystal structures

The β-secretase inhibitor *N*′-[(2*S*,3*R*)-4-(cyclopropylamino)-3-hydroxy-1-phenylbutan-2-yl]-5-(methylsulfonylamino)-*N*-[(1*R*)-1-phenylethyl]benzene-1,3-dicarboxamide (BSIIV) is one of the 5-substituted isophthalamides developed as BACE1 inhibitors by Merck Research Laboratories (Stachel *et al.*, 2004, 2006). BSIIV displays an IC_{50} of 15 n*M* for BACE1 and was found to be tenfold selective for BACE1 *versus* the homologous enzyme BACE2 (Stachel *et al.*, 2004). The crystal structure of a BSIIV–BACE1 complex (PDB entry 2b8l, space group $C222_1$) has been determined for a BACE1 crystal in which a lower affinity inhibitor had been displaced by BSIIV (Stachel *et al.*, 2006).

Here, we report two crystal structures of the BSIIV–BACE1 complex that were obtained from crystals belonging to two

Table 2
Direct and indirect hydrogen bonds between the inhibitor and the enzyme in the three BSIIV–BACE1 crystal structures.

Indirect hydrogen bonds involve a bridging water molecule.

		Cocrystal ($C222_1$)	Soaking ($P6_122$)	2b8l ($C222_1$)
Direct hydrogen bond	Gly34	1	1	1
	Thr72			1
	Gln73	2		1
	Asp228	1	1	1
	Gly230	2	1	2
	Thr232	2	1	
	Asn233	1	2	1
Indirect hydrogen bond	Thr232	1		1
	Arg235	2	2	
	Ser325	1	2	
	Gln326	1	2	

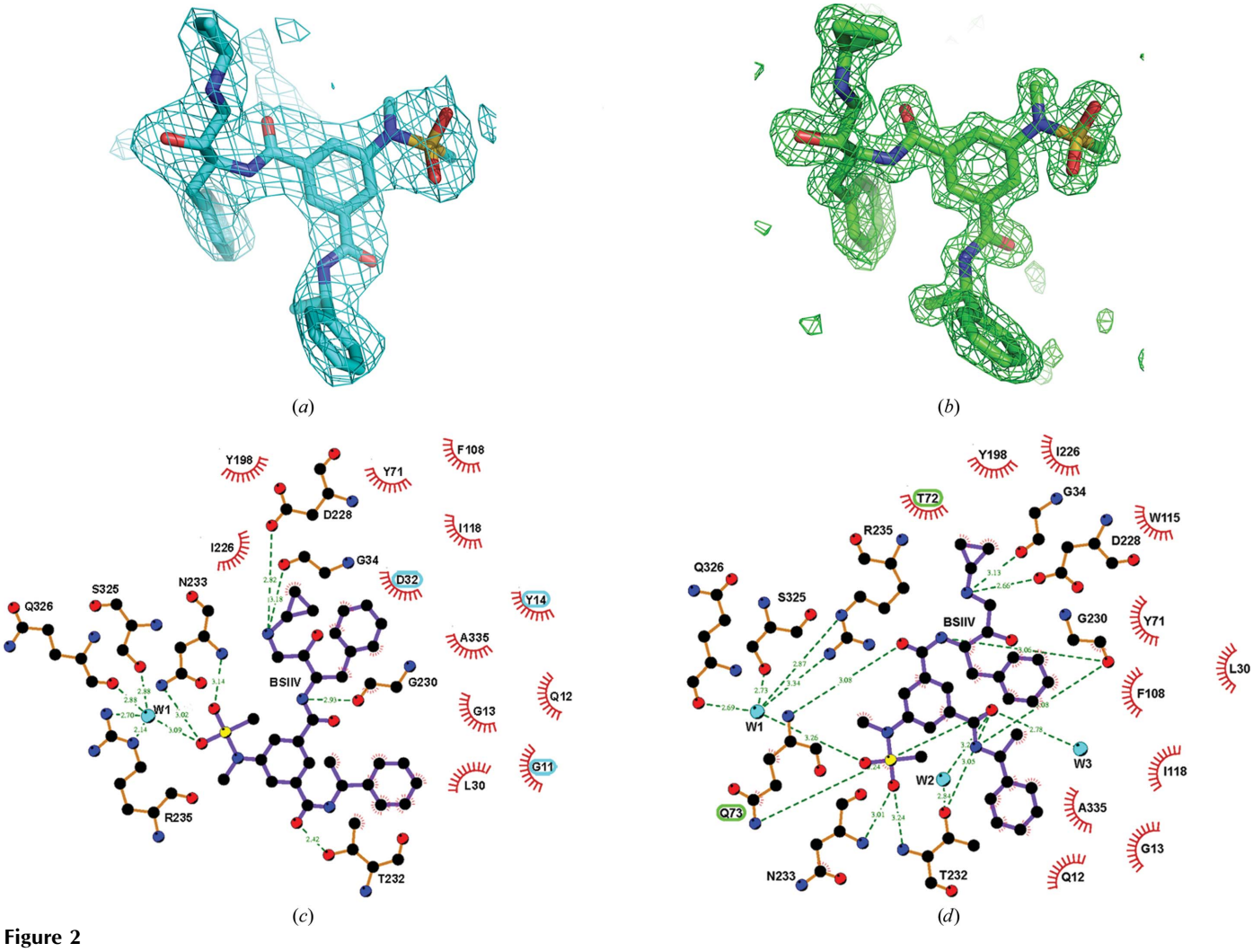

Figure 2
Conformations of BSIIV in the soaked and cocrystallized complexes. (*a*, *b*) ($F_o - F_c$) difference electron-density maps contoured at 3.0σ for BSIIV in the soaked (*a*) and cocrystallized (*b*) structures. (*c*, *d*) *LIGPLOT* representations of the interactions of BSIIV with the enzyme in the soaked (*c*) and cocrystallized (*d*) structures.

different space groups. We obtained crystals of the apo enzyme belonging to space group $P6_122$ and collected a fresh data set in order to exclude the influences of different protein sequences, purification protocols, crystallization conditions and structure-refinement procedures on the crystal structure obtained. Because the final apo BACE1 structure that we obtained was very similar to that of the previously deposited apo structure belonging to the same space group (PDB entry 1w50), neither the data nor the structure are shown here. The first crystalline complex was obtained by soaking BSIIV into a hexagonal apo BACE1 crystal and diffracted to 2.55 Å resolution, compared with 2.3 Å for a data set collected from a crystal of the apo enzyme. The BSIIV structure could be fitted very well into the experimental electron density (Fig. 2*a*). *LIGPLOT* shows that BSIIV forms hydrogen bonds to residues Gly34, Asp228, Gly230, Thr232 and Asn233 (Table 2) and makes hydrophobic interactions with Gly11, Gln12, Gly13, Tyr14, Leu30, Asp32, Tyr71, Phe108, Ile118, Tyr198, Ile226 and Ala335 (Fig. 2*c*). BSIIV also interacts with Arg235, Ser325 and Gln326 *via* a water molecule. No hydrogen bonds are formed between BSIIV and the flap residues, but the inhibitor is seen to make a weak hydrophobic interaction with Tyr71. The structure of the complex thus differs from that reported previously (PDB entry 2b8l), in which hydrogen bonds are formed between the inhibitor and residues Thr72 and Gln73 (Table 2 and Fig. S1). Superposition of the three-dimensional structures (Fig. 3) shows that the conformation of the flap in the structure obtained by soaking in the ligand differs from both that in the apo enzyme structure (PDB entry 1w50) and that in the structure of the complex deposited previously (PDB entry 2b8l). While in the apo structure the flap adopts an open conformation, a closed conformation is seen in the 2b8l structure in which the flap moves closer to the Asp dyad, thus interacting directly with the bound BSIIV. In the soaked structure reported here the flap assumes a conformation intermediate between the open and the closed conformations and forms no direct hydrogen bonds to BSIIV.

Although the flap adopts different conformations in 2b8l and in our soaked structure, the position and orientation of the bound BSIIV in the two structures is almost identical. This led us to attempt to obtain an additional BSIIV–BACE1 crystal structure for comparison, which we were able to do by cocrystallization under conditions that differed from those in which the apo crystals were obtained into which we had soaked the BSIIV. High-quality crystals appeared in hanging drops obtained by mixing a solution of the BSIIV–BACE1 complex with 1.5–1.8 *M* Li_2SO_4, 100 m*M* HEPES pH 7.5. The crystal used to obtain the 2b8l data set had also been grown under these conditions, but through soaking exchange in which a lower affinity ligand had been displaced from the crystals and not by direct cocrystallization. The cocrystals that we obtained belonged to space group $C222_1$ and diffracted to 1.6 Å resolution. The location of the bound BSIIV in the cocrystal structure is very similar to that in the structure obtained by soaking in the ligand and is almost identical to that in 2b8l (Fig. 3). All of the interactions between the protein and inhibitor observed in the soaked structure are conserved in the cocrystallized structure, but two additional hydrogen bonds are formed between BSIIV and Gln73 (Table 2, Figs. 2*b* and 2*d*). Moreover, more hydrogen bonds are formed between the ligand and the protein in our cocrystallized structure than in 2b8l. BSIIV forms one and two more hydrogen bonds with Gln73 and Thr232, respectively, in the cocrystallized structure than in 2b8l. It also forms indirect hydrogen bonds to Arg235, Ser325 and Gln326 *via* a single water molecule. However, whereas BSIIV makes a hydrogen bond with Thr72 in 2b8l, it interacts hydrophobically with the same residue in the cocrystallized structure. The flap in the cocrystallized structure adopts a closed conformation that is similar to that in 2b8l but different from that in the soaked structure (Fig. 3). Not only the flap but also the 10S loop (near residue Ser10) and the 113S loop (near residue Ser113) adopt a more closed conformation both in the cocrystallized structure and in 2b8l than in the soaked structure (Fig. 3).

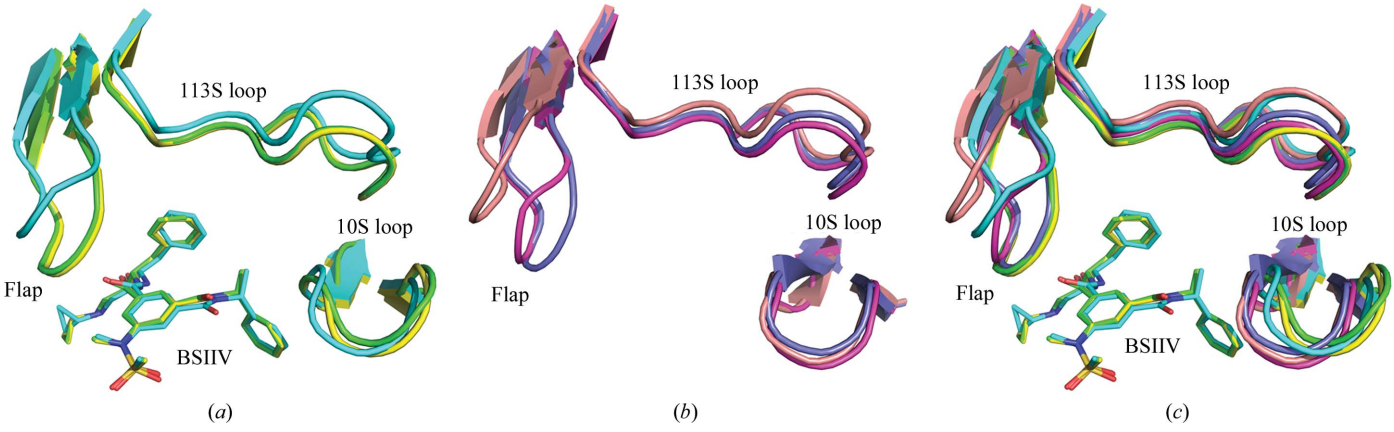

Figure 3
Superimposition of six crystal structures of BACE1. Only the bound ligand and the three loops including residues 5–16, 67–77 and 105–117 are shown. (*a*) The BSIIV complex obtained by cocrystallization (green), the BSIIV complex obtained by soaking (cyan) and the previously deposited BSIIV–BACE1 structure, also obtained by soaking (PDB entry 2b8l; yellow). (*b*) Apo enzymes: Apo1 structure (magenta), Apo2 structure (purple) and the previously deposited apo structure of BACE1 (PDB entry 1w50; light pink). (*c*) Superimposition of the six structures shown in (*a*) and (*b*).

The different conformations of the flap are observed not only in the crystal structures of the two complexes with the same inhibitor but also in the two novel apo structures that we obtained (Fig. 3). The crystals used for the determination of these apo structures were obtained in attempts to cocrystallize a low-affinity inhibitor with BACE1, which resulted in crystal structures that were devoid of the inhibitor in both cases. The Apo1 crystals were obtained using the same precipitant solution as was used to obtain the cocrystals of BSIIV–BACE1 and crystallized in the same space group, $C222_1$. The Apo2 structure was determined with a crystal grown in a different precipitant solution and with a different crystal-packing pattern (space group $C2$; Table 1). Thus, the two apo structures belong to two space groups, $C222_1$ and $C2$, for which structures have not previously been deposited in the PDB nor reported in the literature for BACE1. Superimposition of the two apo structures onto the two complex structures and onto the previously deposited apo structure (PDB entry 1w50) shows that the extent of opening of the flap in the five structures ranges from being largest in 1w50, through the soaked structure, Apo1 and Apo2, to being smallest in the cocrystallized structure (Fig. 3*c*). With respect to the four structures that we report, the conformation of the flap partially overlaps in the soaked and Apo1 structures and almost fully overlaps in the Apo2 and cocrystal structures.

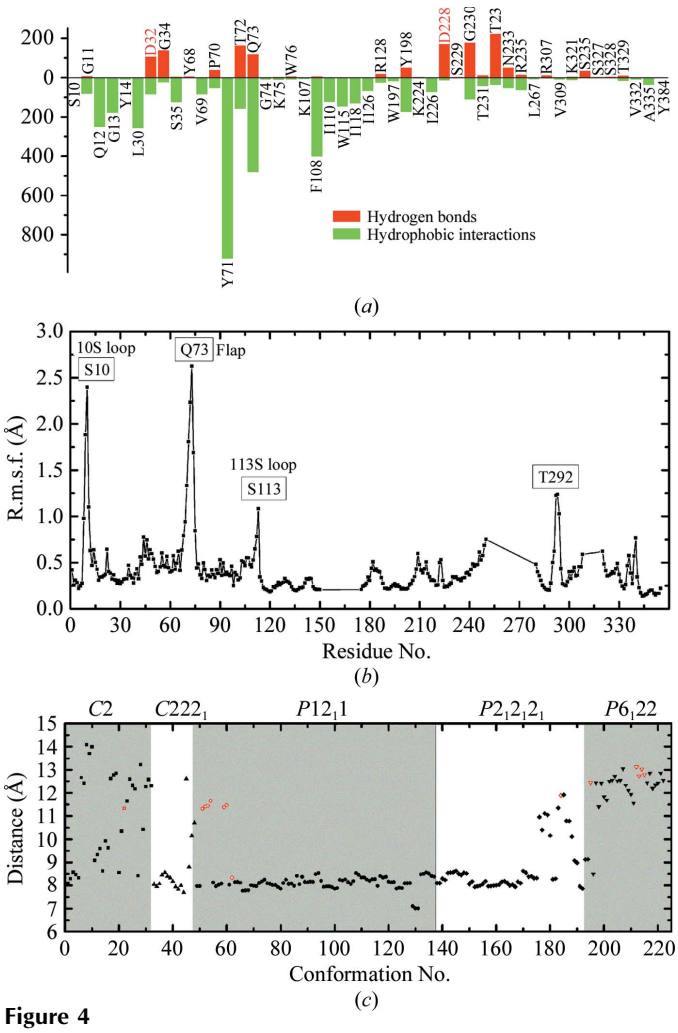

Figure 4
Statistical analyses of the 145 BACE1 data sets deposited in the PDB. (*a*) Hydrogen-bond (red) and hydrophobic (green) interactions between ligands and amino-acid residues in the 208 different BACE1 complex structures. The numbers of hydrogen-bond and hydrophobic interactions were assessed using *LIGPLOT*. (*b*) R.m.s.f. values for the main-chain atoms of the individual amino-acid residues in BACE1 calculated on the basis of the 222 available apo and complex structures extracted from the 145 BACE1 data sets. (*c*) The minimal distance between the C^{α} atoms of flap residues 67–75 and the two carboxyl O atoms of Asp228 in the 208 complex (black) and 14 apo (red) conformations of BACE1. The structures are grouped according to the space groups to which they belong.

3.2. Analysis of crystal structures

Since the first crystal structure of BACE1 was reported, complexed with the octapeptide inhibitor OM99-2 (Hong *et al.*, 2000), more than 100 structures of the native enzyme or of inhibitor complexes have been deposited in the PDB. This is primarily a consequence of the strong pharmaceutical interest in the development of a drug for treatment of AD. Systematic analysis of these structures can yield valuable information that is pertinent to the structure-based design of novel BACE1 inhibitors.

Accordingly, we used the program *LIGPLOT* to analyze the hydrogen-bond and hydrophobic interactions between BACE1 and the various ligands in the 208 conformations of complexes and the data obtained are summarized in Fig. 4(*a*). In addition to the two catalytic residues, Asp32 and Asp228, residues Gly34, Pro70, Thr72, Gln73, Tyr198, Gly230, Thr232, Asn233 and Ser325 frequently form direct hydrogen bond(s) to the peptides, peptoids and other small organic ligands. Residues Gly11, Gln12, Gly13, Leu30, Asp32, Ser35, Val69, Tyr71, Thr72, Gln73, Phe108, Ile110, Trp115, Ile118, Ile126, Tyr198, Ile226 and Gly230 often contribute to hydrophobic ligand–protein interactions. Of the residues in the flap, Thr72 and Gln73 frequently form hydrogen bonds to the ligand, and Tyr71 and Gln73 often make hydrophobic interactions with the ligand, as is the case in our cocrystallized complex structure. Notably, Tyr71 has the highest tendency to interact hydrophobically with the ligand, partially *via* its large aromatic side chain.

The side-chain conformations of residue Tyr71 were examined in more detail owing to its potential self-inhibitory role. Seven groups are seen in the χ_1/χ_2 plot of the side chain of Tyr71 for the 222 conformations extracted from 145 PDB entries for BACE1 (Fig. S2). The χ_1 value for Tyr71 in the majority of the structures is $\sim$300°, and the densest cluster, group *A*, is located in the top right-hand corner with χ_1 and χ_2 values of $\sim$300° and $\sim$270°, respectively. The conformations of Tyr71 in our cocrystallized and soaked structures belonged to groups *a* and *b*, respectively. Owing to the high flexibility of the flap, which is discussed in detail below, shifts in the position and/or orientation of the entire residue, combined with the changes in the χ_1 and χ_2 angles, result in a broad spectrum of conformations of Tyr71. Fig. 4(*a*) shows that Tyr71 is a major contributor to the hydrophobic interaction between the enzyme and the inhibitors in the complexes for which crystal

Table 3
Matthews coefficients, solvent contents and interfacial areas for BACE crystal structures belonging to different space groups.

Space group	Z	Matthews coefficient (Å^3 Da^{-1})	Solvent content (%)	PDB code	Area of interface near flap† (Å^2)	Area of interface around one chain in asymmetric unit† (Å^2)	Overall area of interface in asymmetric unit† (Å^2)
$C2$	4	2.22	44	2iqg (Maillard *et al.*, 2007)	0	2103	2103
	12	2.87	57	3msj (Madden *et al.*, 2010)	719.8	1384	4152
$C222_1$	8	3.00	59	2b8l (Stachel *et al.*, 2006)	512.9	2403.9	2403.9
$P12_11$	4	2.87	57	1fkn (Hong *et al.*, 2000)	222.6	1130.2	2260.4
	6	3.22	62	3duy (Machauer *et al.*, 2009)	430.2/400.2/334.6	957	2871
	8	2.87	58	2g94 (Ghosh *et al.*, 2006)	407.4/216.8	1093.4	4373.6
$P2_12_12_1$	4	2.33	47	2vij (Beswick *et al.*, 2008)	0	1406.9	1406.9
	8	2.94	58	2qp8 (Iserloh *et al.*, 2008)	188.1	1012.3	2024.6
$P6_122$	12	2.99	59	1w50 (Patel *et al.*, 2004)	1690.6	2803.9	2803.9

† Only interfaces with an area above 100 Å^2 were analyzed.

structures have been studied. Thus, its flexibility and the range of conformations that it can adapt need to be taken into consideration in the design of new BACE1 inhibitors.

The root-mean-square fluctuations (r.m.s.f.s) for all of the residues in BACE1 were calculated based on the same set of 222 conformations considered in Fig. S2. Only the main-chain atoms were included in the calculation. Fig. 4(*b*) shows that the r.m.s.f. values for the flap, *i.e.* for Gln73 and the residues around it, are the largest and that residues in the 10S and 113S loops also display high r.m.s.f. values. These data are consistent with the conformational differences that we observe in these regions when comparing our apo, soaked and cocrystallized structures (Fig. 3).

In order to assess the extent of opening of the flap in the different crystal structures, the minimal distance between the C$^\alpha$ atoms of flap residues 67–75 and the two carboxyl O atoms of Asp228 (see Fig. 1*a*) was calculated for all apo and complex BACE1 structures (Fig. 4*c*). From the r.m.s.f. values plotted in Fig. 4(*b*), it is apparent that the positions of Asp228 and its companion dyad member Asp32 are quite fixed in all of the crystal structures. Any change in the distance between them and the flap must thus be a consequence of either a conformational change in the flap or its movement. Five space groups are represented: $P6_122$, $P12_11$, $P2_12_12_1$, $C222_1$ and $C2$. In all of the crystal structures belonging to space group $P12_11$ and in most of those belonging to $P2_12_12_1$ and $C222_1$ this distance is ∼8 Å. Both 2b8l and our cocrystallized complex structure belong to space group $C222_1$ and display similar distances of ∼8 Å. However, in our soaked complex, which belongs to space group $P6_122$, the flap is more open, with a distance of 11 Å. With the exception of 1w51 (Patel *et al.*, 2004), all of the crystal structures of complexes belonging to space group $P6_122$ display a larger distance of ∼12 Å, which is very similar to the distances observed for the apo structures that belong to this same space group (Fig. 4*c*). In the structures of complexes belonging to space group $C2$ the distance between the flap and Asp228 is variable, ranging from 8 to >15 Å. In the 14 apo conformations, which belong to four different space groups, all the distances are above 10 Å except for one copy in PDB entry 1xn3, which belongs to space group $P2_12_12_1$. Our two apo structures, Apo1 (space group $C222_1$) and Apo2 (space group $C2$), also display closed flap conformations, with flap–Asp228 distances of 9 and 8 Å, respectively. In summary, the flap adopts an open conformation in almost all of the apo conformations except for the conformation of one copy in 1xn3 and our two apo structures, and both closed and open conformations are observed in the crystal structures of the complexes.

The various conformations of the flap observed in the apo structures and in those of the complexes and, in particular, the repertoire of conformations that it adopts in structures of complexes belonging to either the same or different space groups raises the issue of the factor(s) that are responsible for these differences. Since the BACE1 crystals generated by us and by others possess different unit cells and belong to several space groups, it was important to assess the possible effect of crystal packing on the observed conformations. The Matthews coefficient (V_M) and solvent content of each crystal structure were calculated using the Protein Function Discovery and Department of Biomedical and Molecular Sciences Molecular Modelling and Crystallographic Computing Facility server at Queen's University (http://pldserver1.biochem.queensu.ca/~rlc/pfd/links/calcs/vm_calc.shtml; Table S1). Since structures with similar unit-cell size belonging to the same space group have very similar V_M values, the averaged V_M and solvent content of the structures belonging to the same space group and with the same Z number (the copy number of BACE1 in the unit cell) are shown in Table 3. We also used the *PDBePISA* server (http://www.ebi.ac.uk/msd-srv/prot_int/) to analyze the areas of the interfaces between the copies of BACE1 for nine PDB depositions (Table 3). Only interfaces with an area of >100 A^2 were visually inspected. The two copies that form the interface adjacent to the flap in the nine structures are shown in Fig. S1 and the areas calculated for these interfaces are shown in Table 3. It can be seen that in structures with low V_M and solvent content, such as 2iqg and 2vij, there is no interface between symmetry-related copies adjacent to the flap region. This suggests that crystal packing does not affect the conformational state of the flap in these structures. Amongst all of the interfaces that are adjacent to the flap, that observed in 1w50, which belongs to space group $P6_122$, has a significantly larger area than the others. Furthermore, the packing of the two copies buries most of the flap region in the 1w50 structure

compared with the others (Fig. S1). It is thus concluded that the effect of crystal packing on the flap in the structures belonging to space group $P6_122$ is the most significant. An open conformation of the flap is observed in all of the apo structures except three, while in the majority of the crystal structures of complexes a closed conformation is adopted. This suggests that in general the binding of the ligand induces the transition to a closed conformation. However, an open conformation is observed in the structures of quite a few complexes, including all but one of those belonging to space group $P6_122$ (Figs. 4*c* and 5*a*). In all the other $P6_122$ structures the flap is open and is not in direct contact with the bound inhibitor.

Inspection of the pattern of hydrogen-bond interactions using *LIGPLOT* (Fig. 2) shows that in complexes in which the flap is in an open conformation there are no hydrogen bonds between the main chain of the flap residues and the inhibitor. Conversely, inspection of the structures with a closed flap always reveals at least one such hydrogen bond between the flap and the inhibitor. Thus, hydrogen-bond formation between the main chain of the flap residues and the bound ligand is a major force driving the flap into a closed conformation. When the flap adopts an open conformation, this can sometimes be ascribed to the position and/or orientation of the bound ligand. For example, in the 2q15 structure, which belongs to space group $P6_122$, the inhibitor protrudes in such a way as to sterically prevent the flap from closing (Fig. 5*a*, purple structure). Similar cases are seen in crystal structures belonging to space groups $C222_1$, $C2$ and $P2_12_12_1$ (Figs. 5*b*, 5*c* and 5*d*). Interestingly, an open flap without bound ligand, an open flap with bound ligand and a closed flap with bound ligand are seen side by side in the three molecules in the asymmetric unit of a single structure (PDB entry 3hvg, space group $C2$; Fig. 5*e*). In copy *A* (green) the inhibitor hydrogen bonds directly to the main chain of the flap, producing a closed conformation. In copy *B* (cyan) the inhibitor is bound at the

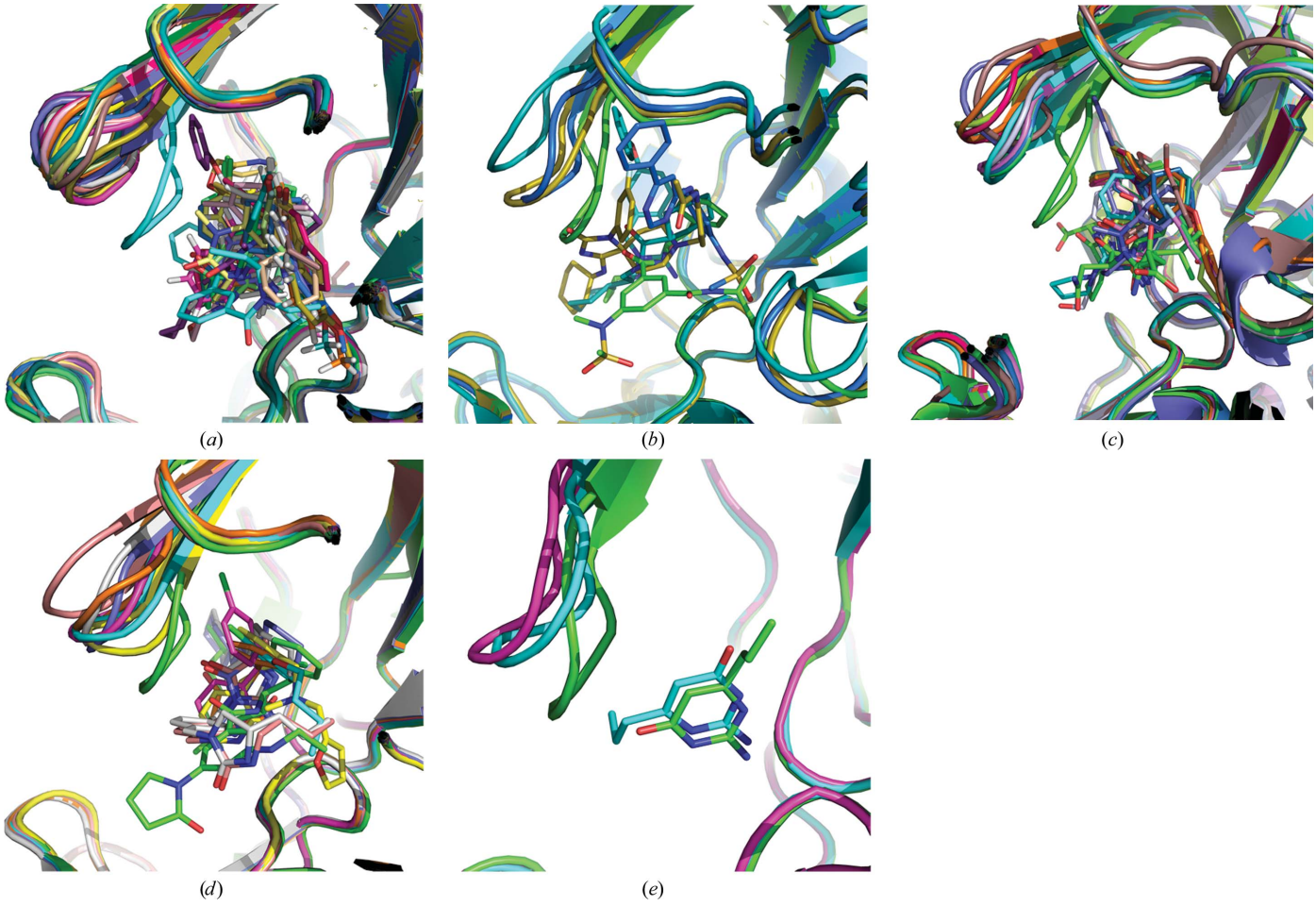

Figure 5
Superpositions of ribbon representations of the area around the flap in ligand–BACE1 complexes with open flap conformations crystallizing in different space groups. For comparison, a BACE1 structure with a closed flap is displayed in each representation. (*a*) Superimposition of all of the BACE1 complexes that crystallized in space group $P6_122$. The cyan and purple structures represent PDB entries 1w51 and 2q15, respectively. (*b*) Superimposition of structures belonging to space group $C222_1$: PDB entries 3fkt (yellow), 3exo (blue), 2wjo (cyan) and our cocrystallized structure (green). (*c*) Superimposition of structures belonging to space group $C121$: PDB entries 1ym4 (green), 2a11 (purple), 2qu2, 2qu3, 2zdz, 3hw1, 3h0b, 3in3, 3ind, 3l3a, 3lhg and 3msj. (*d*) Superimposition of structures belonging to space group $P2_12_12_1$: PDB entries 2vie (green), 3kmx, 3kmy, 3kn0, 3l5d, 3l5e, 3l5f and 3l59. (*e*) Superimposition of the three copies in the asymmetric unit of PDB entry 3hvg belonging to space group $C2$: chain *A* (green), chain *B* (cyan) and chain *C* (magenta). In all cases the inhibitors are displayed as stick models.

same position but in a different orientation which precludes hydrogen-bond formation between the flap and the inhibitor and results in an open conformation. In copy *C* (magenta) no bound inhibitor is seen and the flap is open. In summary, direct hydrogen-bond interaction between the main chain of the flap residues and the inhibitor and the position and/or the orientation of the inhibitor are the factors that determine the conformation of the flap in the crystal structures of BACE1 complexes.

3.3. MD simulations

The open flap conformation observed in our soaked structure as well as in all but one of the crystal structures of BACE1 complexes belonging to space group $P6_122$ that have been deposited in the PDB led us to speculate that the crystal-packing pattern of the enzyme within this space group may affect the conformation of the flap. MD simulations were performed in order to examine this possibility. Two models were selected: a monomer and a 'dimer'. The only molecule in the asymmetric unit of PDB entry 1w50 (space group $P6_122$) was selected as the monomer model. The 'dimer' was constructed using the same structure by taking the single molecule present in the asymmetric unit together with a crystallographic symmetry-related copy (Fig. 1*b*). It is apparent that the flaps in the two copies of this 'dimer' face each other.

The r.m.s.d.s for C^{α} atoms shown in Fig. 6(*a*) indicate that the stability of the whole BACE1 molecule in the monomer and in both copies of the 'dimer' are similar during the 500 ns simulation period, since most of the r.m.s.d.s in either the monomer or the 'dimer' are in the range 2–2.5 Å. However, the minimal distance between the C^{α} atoms of flap residues 67–75 and the two carboxyl O atoms of Asp228 in each monomer of the 'dimer' is generally larger than in the monomer (Fig. 6*b*). In the monomer (black curve) the distance is ∼10 Å and its fluctuations are more limited than those seen for either copy of the 'dimer'. In one monomer of the 'dimer' (green curve) the distance between the flap and Asp228 fluctuates around 13 Å during the 500 ns simulation period, while in the second monomer (red curve) its value dropped to ∼7.5 Å during the first ∼70 ns; it then increased to and remained at ∼17 Å for ∼200 ns and finally decreased again to ∼11 Å during the last ∼150 ns. Thus, the flap in both monomers of the 'dimer' appears to be in an open conformation during most of the simulation time. This is in agreement with our observation that in all of the crystal structures belonging to space group $P6_122$ except one (Figs. 4*c* and 5*a*) the degree of opening of the flap and the extent to which it resides in the open conformation are both larger in the artificial 'dimer' than in the monomer. We thus speculate that the crystal-packing pattern in space group $P6_122$ may favour a more open conformation.

4. Discussion

In the present study, four new crystal structures were determined: that of a BSIIV–BACE1 complex belonging to space group $P6_122$, those of a second BSIIV–BACE1 complex and of an apo structure both belonging to space group $C222_1$, and that of a second apo structure belonging to space group $C2$. The crystals of the BSIIV complex belonging to space group $P6_122$ were obtained by soaking the inhibitor into a crystal of the apo enzyme belonging to the same space group, while those of the complex belonging to space group $C222_1$ were obtained by cocrystallization of the inhibitor and the enzyme. The two apo structures belonging to different space groups were obtained by cocrystallization in the presence of another low-affinity inhibitor using two different precipitants; in both cases the inhibitor was not observed in the crystals thus obtained. Surprisingly, even though the inhibitor is bound at almost identical loci in the two complexes, the conformations of the residues surrounding it are not identical (Fig. 3). Superimposition of the structures of the two apo enzymes and

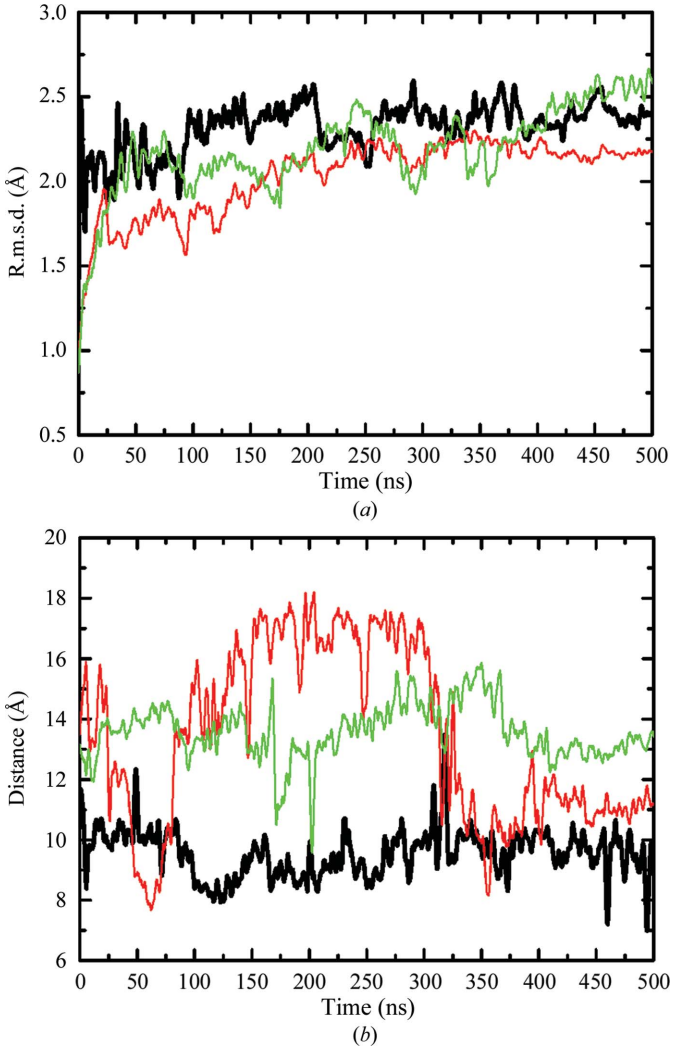

Figure 6
MD simulations of the BACE1 monomer and 'dimer'. (*a*) Time-dependent r.m.s.d.s of the C^{α} atoms with respect to their starting positions in the trajectories of BACE1 in the monomer (black) and in the two copies of the 'dimer' (red and green). (*b*) Time-dependence of the distances between the C^{α} atoms of flap residues 67–75 and the two carboxyl O atoms of Asp228 in the monomer (black) and in the two copies of BACE1 in the 'dimer' (green and red).

of the two complexes revealed that the flap (residues 67–75) that folds over the active site adopts a different conformation in each of them. This led us to carry out a systematic analysis of all of the BACE1 crystal structures deposited in the PDB (both apo structures and complexes) and to perform MD simulations on the apo enzyme in order to investigate the underlying causes for the various conformations adopted by the flap. In particular, we wished to clarify whether they might be a consequence of crystal packing in different space groups or might indicate that the active site can assume multiple low-energy conformations. The r.m.s.f.s of main-chain atoms calculated based on all of the BACE1 crystal structures deposited in the PDB show that the flap is the most flexible region of the protein. The minimal distance between the flap residues and the catalytic residue Asp228, which provides a measure of the extent of opening of the flap, reveals that the flap adopts an open conformation in all the apo structures with two exceptions; not surprisingly, the situation with respect to the structures of the complexes is more complex. In most of the complexes, direct hydrogen-bonding interactions between main-chain atoms of flap residues and the bound inhibitor lock the flap in the closed conformation, except in a few cases in which the position and orientation of the inhibitors sterically preclude its closing. It is of interest that no direct hydrogen bonds are formed between the inhibitor and the flap in complexes in which the flap is in an open conformation, as is the case in the crystal structure of the complex that we obtained by soaking BSIIV into apo crystals of BACE1, but a direct hydrogen bond between Gln73 and BSIIV locks the flap in a closed conformation in the cocrystallized structure. It may thus be concluded that the formation of a direct hydrogen bond between a main-chain atom of a flap residue and the bound inhibitor is a prerequisite for the flap to assume a closed conformation in a complex. Interestingly, in all of the crystal structures of complexes that belong to space group $P6_122$ except one, the flap is in an open conformation. Our soaked crystals of the BSIIV–BACE1 complex also belonged to space group $P6_122$. Analysis of the crystal-packing pattern revealed that in this space group the flap is at a packing interface. MD simulations were carried out to check whether the observed packing would influence the conformation of the flap. In a starting model for MD that includes a symmetry-related copy of BACE1 both the degree of opening and the time that the flap dwells in the open state are much larger than in the trajectories generated for the monomer. Thus, the packing pattern in crystals belonging to space group $P6_122$ hinders conformational change in the flap, which may be the main reason why in our BSIIV–BACE1 complex belonging to space group $P6_122$ the bound BSIIV does not cause the flap to adopt a closed conformation, whereas it does so in the complex belonging to space group $C222_1$.

In summary, the multiple conformations of the active-site region of BACE1, and in particular of the flap, displayed in the various crystal structures reveal the high flexibility of the enzyme, which is consistent with the fact that aspartic proteases often employ conformational changes to modulate their intrinsic activity (James *et al.*, 1982; Sali *et al.*, 1992; Andreeva & Rumsh, 2001; Hornak *et al.*, 2006; Eder *et al.*, 2007). The interaction between the inhibitor and the flap residues, the binding site of the inhibitor and the space group all influence the conformation adopted by the flap. Consideration of these issues should assist in the design of novel and more effective BACE1 inhibitors.

5. Conclusions

Crystal structure determination and analysis and MD simulations were performed to study the structure–function relationships in the potentially important anti-AD drug target BACE1. It was found that the conformations of the enzyme in two different crystal structures of complexes of the enzyme with the same inhibitor, as well as in two apo structures, differ significantly, particularly in the active-site flap and in the 10S and 113S loops. Detailed analysis of all of the crystal structures of BACE1 deposited in the PDB revealed that flexibility of all three of these regions is a general phenomenon. In particular, the multiple conformations assumed by the flap, which are tightly associated with catalytic function, are influenced by the presence, position and orientation of a bound inhibitor. An open conformation of the flap is often observed in the apo structures, while direct hydrogen-bonding interaction between main-chain atoms of the flap and the inhibitor is a prerequisite for the flap to adopt a closed conformation in the crystal structures of complexes. Detailed examination of the conformational changes occurring in BACE1 thus highlights the flexibility of the flap as well as the different binding modalities of the various inhibitors. These factors need to be taken into account in the design of new BACE1 inhibitors that may serve as lead compounds for the development of an effective drug for the treatment of AD. Study of the conformational flexibility of the enzyme should not only contribute to structure-based drug design related to BACE1, as well as to other targets with flexible conformations, but should also enhance our understanding of the mechanistic events associated with the binding of substrates and inhibitors to the enzyme.

This study was supported by the '100 Talents Project' of CAS (to YX), the Shanghai Pujiang Program (Grant No. 10PJ1412000), the National Natural Science Foundation of China (Grant No. 20720102040), the State Key Program of Basic Research of China (Grant No. 2009CB918501), the Israel Science Foundation, the European Commission VIth Framework Research and Technological Development Program 'SPINE2-COMPLEXES' Project under contract No. 031220 and 'Teach-SG' Project under contract No. ISSG-CT-2007-037198, the Kimmelman Center for Biomolecular Structure and Assembly, the Benoziyo Center for Neurosciences, the Divadol Foundation, the Nalvyco Foundation, the Bruce Rosen Foundation and the Lurman & Garoon Foundation. JLS is the Morton and Gladys Pickman Professor of Structural Biology. Computation resources were supported by the Computer Network Information Center (CNIC), Chinese Academy of Sciences (CAS) and Shanghai Super-

computing Center (SCC) and were sponsored by a grant from the Information Construction Project of the Chinese Academy of Sciences during the 11th Five-Year Plan Period.

References

Adams, P. D., Grosse-Kunstleve, R. W., Hung, L.-W., Ioerger, T. R., McCoy, A. J., Moriarty, N. W., Read, R. J., Sacchettini, J. C., Sauter, N. K. & Terwilliger, T. C. (2002). *Acta Cryst.* D**58**, 1948–1954.

Andreeva, N. S. & Rumsh, L. D. (2001). *Protein Sci.* **10**, 2439–2450.

Bäck, M., Nyhlén, J., Kvarnström, I., Appelgren, S., Borkakoti, N., Jansson, K., Lindberg, J., Nyström, S., Hallberg, A., Rosenquist, S. & Samuelsson, B. (2008). *Bioorg. Med. Chem.* **16**, 9471–9486.

Barrow, J. C., Rittle, K. E., Ngo, P. L., Selnick, H. G., Graham, S. L., Pitzenberger, S. M., McGaughey, G. B., Colussi, D., Lai, M. T., Huang, Q., Tugusheva, K., Espeseth, A. S., Simon, A. J., Munshi, S. K. & Vacca, J. P. (2007). *ChemMedChem*, **2**, 995–999.

Barrow, J. C., Stauffer, S. R. *et al.* (2008). *J. Med. Chem.* **51**, 6259–6262.

Baxter, E. W. *et al.* (2007). *J. Med. Chem.* **50**, 4261–4264.

Berendsen, H. J. C., van der Spoel, D. & van Drunen, R. (1995). *Comput. Phys. Commun.* **91**, 43–56.

Beswick, P. *et al.* (2008). *Bioorg. Med. Chem. Lett.* **18**, 1022–1026.

Björklund, C., Adolfsson, H., Jansson, K., Lindberg, J., Vrang, L., Hallberg, A., Rosenquist, S. & Samuelsson, B. (2010). *Bioorg. Med. Chem.* **18**, 1711–1723.

Björklund, C., Oscarson, S., Benkestock, K., Borkakoti, N., Jansson, K., Lindberg, J., Vrang, L., Hallberg, A., Rosenquist, A. & Samuelsson, B. (2010). *J. Med. Chem.* **53**, 1458–1464.

Cai, H., Wang, Y., McCarthy, D., Wen, H., Borchelt, D. R., Price, D. L. & Wong, P. C. (2001). *Nature Neurosci.* **4**, 233–234.

Cascella, M., Micheletti, C., Rothlisberger, U. & Carloni, P. (2005). *J. Am. Chem. Soc.* **127**, 3734–3742.

Charrier, N. *et al.* (2008). *J. Med. Chem.* **51**, 3313–3317.

Charrier, N., Clarke, B., Cutler, L. *et al.* (2009*a*). *Bioorg. Med. Chem. Lett.* **19**, 3664–3668.

Charrier, N., Clarke, B., Cutler, L. *et al.* (2009*b*). *Bioorg. Med. Chem. Lett.* **19**, 3674–3678.

Charrier, N., Clarke, B., Demont, E. *et al.* (2009). *Bioorg. Med. Chem. Lett.* **19**, 3669–3673.

Clarke, B. *et al.* (2008*a*). *Bioorg. Med. Chem. Lett.* **18**, 1011–1016.

Clarke, B. *et al.* (2008*b*). *Bioorg. Med. Chem. Lett.* **18**, 1017–1021.

Clarke, B. *et al.* (2010). *Bioorg. Med. Chem. Lett.* **20**, 4639–4644.

Coburn, C. A. *et al.* (2004). *J. Med. Chem.* **47**, 6117–6119.

Coburn, C. A. *et al.* (2006). *Bioorg. Med. Chem. Lett.* **16**, 3635–3638.

Cole, D. C. *et al.* (2008). *Bioorg. Med. Chem. Lett.* **18**, 1063–1066.

Congreve, M., Aharony, D., Albert, J., Callaghan, O., Campbell, J., Carr, R. A., Chessari, G., Cowan, S., Edwards, P. D., Frederickson, M., McMenamin, R., Murray, C. W., Patel, S. & Wallis, N. (2007). *J. Med. Chem.* **50**, 1124–1132.

Cumming, J. N. *et al.* (2008). *Bioorg. Med. Chem. Lett.* **18**, 3236–3241.

Cumming, J. N. *et al.* (2010). *Bioorg. Med. Chem. Lett.* **20**, 2837–2842.

Duan, Y., Wu, C., Chowdhury, S., Lee, M. C., Xiong, G., Zhang, W., Yang, R., Cieplak, P., Luo, R., Lee, T., Caldwell, J., Wang, J. & Kollman, P. (2003). *J. Comput. Chem.* **24**, 1999–2012.

Eder, J., Hommel, U., Cumin, F., Martoglio, B. & Gerhartz, B. (2007). *Curr. Pharm. Des.* **13**, 271–285.

Edwards, P. D. *et al.* (2007). *J. Med. Chem.* **50**, 5912–5925.

Emsley, P. & Cowtan, K. (2004). *Acta Cryst.* D**60**, 2126–2132.

Esler, W. P. & Wolfe, M. S. (2001). *Science*, **293**, 1449–1454.

Fobare, W. F., Solvibile, W. R., Robichaud, A. J., Malamas, M. S., Manas, E., Turner, J., Hu, Y., Wagner, E., Chopra, R., Cowling, R., Jin, G. & Bard, J. (2007). *Bioorg. Med. Chem. Lett.* **17**, 5353–5356.

Freskos, J. N., Fobian, Y. M., Benson, T. E., Bienkowski, M. J. *et al.* (2007). *Bioorg. Med. Chem. Lett.* **17**, 73–77.

Freskos, J. N., Fobian, Y. M., Benson, T. E., Moon J. B. *et al.* (2007). *Bioorg. Med. Chem. Lett.* **17**, 78–81.

Ghosh, A. K., Devasamudram, T., Hong, L., DeZutter, C., Xu, X., Weerasena, V., Koelsch, G., Bilcer, G. & Tang, J. (2005). *Bioorg. Med. Chem. Lett.* **15**, 15–20.

Ghosh, A. K., Kumaragurubaran, N., Hong, L., Kulkarni, S. S., Xu, X., Chang, W., Weerasena, V., Turner, R., Koelsch, G., Bilcer, G. & Tang, J. (2007). *J. Med. Chem.* **50**, 2399–2407.

Ghosh, A. K., Kumaragurubaran, N., Hong, L., Kulkarni, S., Xu, X., Miller, H. B., Reddy, D. S., Weerasena, V., Turner, R., Chang, W., Koelsch, G. & Tang, J. (2008). *Bioorg. Med. Chem. Lett.* **18**, 1031–1036.

Ghosh, A. K., Kumaragurubaran, N., Hong, L., Lei, H., Hussain, K. A., Liu, C.-F., Devasamudram, T., Weerasena, V., Turner, R., Koelsch, G., Bilcer, G. & Tang, J. (2006). *J. Am. Chem. Soc.* **128**, 5310–5311.

Godemann, R., Madden, J., Krämer, J., Smith, M., Fritz, U., Hesterkamp, T., Barker, J., Höppner, S., Hallett, D., Cesura, A., Ebneth, A. & Kemp, J. (2009). *Biochemistry*, **48**, 10743–10751.

Gorfe, A. A. & Caflisch, A. (2005). *Structure*, **13**, 1487–1498.

Hanessian, S. *et al.* (2005). *J. Med. Chem.* **48**, 5175–5190.

Hanessian, S., Shao, Z., Betschart, C., Rondeau, J. M., Neumann, U. & Tintelnot-Blomley, M. (2010). *Bioorg. Med. Chem. Lett.* **20**, 1924–1927.

Hanessian, S., Yang, G., Rondeau, J. M., Neumann, U., Betschart, C. & Tintelnot-Blomley, M. (2006). *J. Med. Chem.* **49**, 4544–4567.

Hess, B., Kutzner, C., van der Spoel, D. & Lindahl, E. (2008). *J. Chem. Theory Comput.* **4**, 435–447.

Hong, L., Koelsch, G., Lin, X., Wu, S., Terzyan, S., Ghosh, A. K., Zhang, X. C. & Tang, J. (2000). *Science*, **290**, 150–153.

Hong, L. & Tang, J. (2004). *Biochemistry*, **43**, 4689–4695.

Hong, L., Turner, R. T. III, Koelsch, G., Shin, D., Ghosh, A. K. & Tang, J. (2002). *Biochemistry*, **41**, 10963–10967.

Hornak, V., Okur, A., Rizzo, R. C. & Simmerling, C. (2006). *Proc. Natl Acad. Sci. USA*, **103**, 915–920.

Iserloh, U., Pan, J., Stamford, A. W., Kennedy, M. E., Zhang, Q., Zhang, L., Parker, E. M., McHugh, N. A., Favreau, L., Strickland, C. & Voigt, J. (2008). *Bioorg. Med. Chem. Lett.* **18**, 418–422.

Iserloh, U., Wu, Y., Cumming, J. N., Pan, J., Wang, L. Y., Stamford, A. W., Kennedy, M. E., Kuvelkar, R., Chen, X., Parker, E. M., Strickland, C. & Voigt, J. (2008). *Bioorg. Med. Chem. Lett.* **18**, 414–417.

James, M. N., Sielecki, A., Salituro, F., Rich, D. H. & Hofmann, T. (1982). *Proc. Natl Acad. Sci. USA*, **79**, 6137–6141.

Kabsch, W. (2010). *Acta Cryst.* D**66**, 125–132.

Kortum, S. W., Benson, T. E., Bienkowski, M. J., Emmons, T. L., Prince, D. B., Paddock, D. J., Tomasselli, A. G., Moon, J. B., LaBorde, A. & TenBrink, R. E. (2007). *Bioorg. Med. Chem. Lett.* **17**, 3378–3383.

Kuglstatter, A., Stahl, M., Peters, J. U., Huber, W., Stihle, M., Schlatter, D., Benz, J., Ruf, A., Roth, D., Enderle, T. & Hennig, M. (2008). *Bioorg. Med. Chem. Lett.* **18**, 1304–1307.

Lerchner, A., Machauer, R., Betschart, C., Veenstra, S., Rueeger, H., McCarthy, C., Tintelnot-Blomley, M., Jaton, A. L., Rabe, S., Desrayaud, S., Enz, A., Staufenbiel, M., Paganetti, P., Rondeau, J. M. & Neumann, U. (2010). *Bioorg. Med. Chem. Lett.* **20**, 603–607.

Lin, X., Koelsch, G., Wu, S., Downs, D., Dashti, A. & Tang, J. (2000). *Proc. Natl Acad. Sci. USA*, **97**, 1456–1460.

Lindahl, E., Hess, B. & van der Spoel, D. (2001). *J. Mol. Model.* **7**, 306–317.

Lindsley, S. R. *et al.* (2007). *Bioorg. Med. Chem. Lett.* **17**, 4057–4061.

Luo, Y. *et al.* (2001). *Nature Neurosci.* **4**, 231–232.

Machauer, R., Laumen, K., Veenstra, S., Rondeau, J. M., Tintelnot-Blomley, M., Betschart, C., Jaton, A. L., Desrayaud, S., Staufenbiel, M., Rabe, S., Paganetti, P. & Neumann, U. (2009). *Bioorg. Med. Chem. Lett.* **19**, 1366–1370.

Machauer, R., Veenstra, S., Rondeau, J. M., Tintelnot-Blomley, M., Betschart, C., Neumann, U. & Paganetti, P. (2009). *Bioorg. Med. Chem. Lett.* **19**, 1361–1365.

Madden, J., Dod, J. R., Godemann, R., Kraemer, J., Smith, M., Biniszkiewicz, M., Hallett, D. J., Barker, J., Dyekjaer, J. D. & Hesterkamp, T. (2010). *Bioorg. Med. Chem. Lett.* **20**, 5329–5333.
Maillard, M. C. *et al.* (2007). *J. Med. Chem.* **50**, 776–781.
Malamas, M. S., Barnes, K., Hui, Y. *et al.* (2010). *Bioorg. Med. Chem. Lett.* **20**, 2068–2073.
Malamas, M. S., Barnes, K., Johnson, M. *et al.* (2010). *Bioorg. Med. Chem.* **18**, 630–639.
Malamas, M. S., Erdei, J., Gunawan, I., Barnes, K., Johnson, M., Hui, Y., Turner, J., Hu, Y., Wagner, E., Fan, K., Olland, A., Bard, J. & Robichaud, A. J. (2009). *J. Med. Chem.* **52**, 6314–6323.
Malamas, M. S., Erdei, J., Gunawan, I., Turner, J., Hu, Y., Wagner, E., Fan, K., Chopra, R., Olland, A., Bard, J., Jacobsen, S., Magolda, R. L., Pangalos, M. & Robichaud, A. J. (2010). *J. Med. Chem.* **53**, 1146–1158.
McGaughey, G. B., Colussi, D., Graham, S. L., Lai, M. T., Munshi, S. K., Nantermet, P. G., Pietrak, B., Rajapakse, H. A., Selnick, H. G., Stauffer, S. R. & Holloway, M. K. (2007). *Bioorg. Med. Chem. Lett.* **17**, 1117–1121.
Moore, K. P., Zhu, H., Rajapakse, H. A., McGaughey, G. B., Colussi, D., Price, E. A., Sankaranarayanan, S., Simon, A. J., Pudvah, N. T., Hochman, J. H., Allison, T., Munshi, S. K., Graham, S. L., Vacca, J. P. & Nantermet, P. G. (2007). *Bioorg. Med. Chem. Lett.* **17**, 5831–5835.
Murray, C. W., Callaghan, O., Chessari, G., Cleasby, A., Congreve, M., Frederickson, M., Hartshorn, M. J., McMenamin, R., Patel, S. & Wallis, N. (2007). *J. Med. Chem.* **50**, 1116–1123.
Nicholls, A., McGaughey, G. B., Sheridan, R. P., Good, A. C., Warren, G., Mathieu, M., Muchmore, S. W., Brown, S. P., Grant, J. A., Haigh, J. A., Nevins, N., Jain, A. N. & Kelley, B. (2010). *J. Med. Chem.* **53**, 3862–3886.
Otwinowski, Z. & Minor, W. (1997). *Methods Enzymol.* **276**, 307–326.
Park, H. & Lee, S. (2003). *J. Am. Chem. Soc.* **125**, 16416–16422.
Park, H., Min, K., Kwak, H.-S., Koo, K. D., Lim, D., Seo, S.-W., Choi, J.-U., Platt, B. & Choi, D.-Y. (2008). *Bioorg. Med. Chem. Lett.* **18**, 2900–2904.
Patel, S., Vuillard, L., Cleasby, A., Murray, C. W. & Yon, J. (2004). *J. Mol. Biol.* **343**, 407–416.
Probst, G. D. *et al.* (2010). *Bioorg. Med. Chem. Lett.* **20**, 6034–6039.
Rajapakse, H. A. *et al.* (2006). *J. Med. Chem.* **49**, 7270–7273.
Roberds, S. L. *et al.* (2001). *Hum. Mol. Genet.* **10**, 1317–1324.
Sali, A., Veerapandian, B., Cooper, J. B., Moss, D. S., Hofmann, T. & Blundell, T. L. (1992). *Proteins*, **12**, 158–170.
Sardana, V., Xu, B., Zugay-Murphy, J., Chen, Z., Sardana, M., Darke, P. L., Munshi, S. & Kuo, L. C. (2004). *Protein Expr. Purif.* **34**, 190–196.
Sealy, J. M. *et al.* (2009). *Bioorg. Med. Chem. Lett.* **19**, 6386–6391.
Selkoe, D. J. (1991). *Neuron*, **6**, 487–498.
Shimizu, H., Tosaki, A., Kaneko, K., Hisano, T., Sakurai, T. & Nukina, N. (2008). *Mol. Cell. Biol.* **28**, 3663–3671.
Sinha, S. *et al.* (1999). *Nature (London)*, **402**, 537–540.
Sinha, S. & Lieberburg, I. (1999). *Proc. Natl Acad. Sci. USA*, **96**, 11049–11053.
Stachel, S. J. *et al.* (2004). *J. Med. Chem.* **47**, 6447–6450.
Stachel, S. J. *et al.* (2009). *Bioorg. Med. Chem. Lett.* **19**, 2977–2980.
Stachel, S. J., Coburn, C. A., Steele, T. G., Crouthamel, M. C., Pietrak, B. L., Lai, M. T., Holloway, M. K., Munshi, S. K., Graham, S. L. & Vacca, J. P. (2006). *Bioorg. Med. Chem. Lett.* **16**, 641–644.
Stauffer, S. R. *et al.* (2007). *Bioorg. Med. Chem. Lett.* **17**, 1788–1792.
Steele, T. G., Hills, I. D., Nomland, A. A., de León, P., Allison, T., McGaughey, G., Colussi, D., Tugusheva, K., Haugabook, S. J., Espeseth, A. S., Zuck, P., Graham, S. L. & Stachel, S. J. (2009). *Bioorg. Med. Chem. Lett.* **19**, 17–20.
Truong, A. P. *et al.* (2010). *Bioorg. Med. Chem. Lett.* **20**, 4789–4794.
Turner, R. T. III, Hong, L., Koelsch, G., Ghosh, A. K. & Tang, J. (2005). *Biochemistry*, **44**, 105–112.
Van Der Spoel, D., Lindahl, E., Hess, B., Groenhof, G., Mark, A. E. & Berendsen, H. J. (2005). *J. Comput. Chem.* **26**, 1701–1718.
Vassar, R. (2004). *J. Mol. Neurosci.* **23**, 105–114.
Wallace, A. C., Laskowski, R. A. & Thornton, J. M. (1995). *Protein Eng.* **8**, 127–134.
Wang, Y.-S. *et al.* (2010). *J. Med. Chem.* **53**, 942–950.
Wångsell, F., Gustafsson, K., Kvarnström, I., Borkakoti, N., Edlund, M., Jansson, K., Lindberg, J., Hallberg, A., Rosenquist, A. & Samuelsson, B. (2010). *Eur. J. Med. Chem.* **45**, 870–882.
Wångsell, F., Nordeman, P., Sävmarker, J., Emanuelsson, R., Jansson, K., Lindberg, J., Rosenquist, S., Samuelsson, B. & Larhed, M. (2011). *Bioorg. Med. Chem.* **19**, 145–155.
Winn, M. D. *et al.* (2011). *Acta Cryst.* D**67**, 235–242.
Xiong, B., Huang, X.-Q., Shen, L.-L., Shen, J.-H., Luo, X.-M., Shen, X., Jiang, H.-L. & Chen, K.-X. (2004). *Acta Pharmacol. Sin.* **25**, 705–713.
Xu, Y., Colletier, J.-P., Weik, M., Jiang, H., Moult, J., Silman, I. & Sussman, J. L. (2008). *Biophys. J.* **95**, 2500–2511.
Yan, R., Bienkowski, M. J., Shuck, M. E., Miao, H., Tory, M. C., Pauley, A. M., Brashier, J. R., Stratman, N. C., Mathews, W. R., Buhl, A. E., Carter, D. B., Tomasselli, A. G., Parodi, L. A., Heinrikson, R. L. & Gurney, M. E. (1999). *Nature (London)*, **402**, 533–537.
Yang, W. *et al.* (2009). *Biochemistry*, **48**, 4488–4496.
Yang, W., Lu, W., Lu, Y., Zhong, M., Sun, J., Thomas, A. E., Wilkinson, J. M., Fucini, R. V., Lam, M., Randal, M., Shi, X. P., Jacobs, J. W., McDowell, R. S., Gordon, E. M. & Ballinger, M. D. (2006). *J. Med. Chem.* **49**, 839–842.
Zhou, P., Li, Y., Fan, Y., Wang, Z., Chopra, R., Olland, A., Hu, Y., Magolda, R. L., Pangalos, M., Reinhart, P. H., Turner, M. J., Bard, J., Malamas, M. S. & Robichaud, A. J. (2010). *Bioorg. Med. Chem. Lett.* **20**, 2326–2329.
Zhu, Z. *et al.* (2010). *J. Med. Chem.* **53**, 951–965.